We are IntechOpen, the world's leading publisher of Open Access books Built by scientists, for scientists

4,800
Open access books available

122,000
International authors and editors

135M
Downloads

Our authors are among the

154
Countries delivered to

TOP 1%
most cited scientists

12.2%
Contributors from top 500 universities

WEB OF SCIENCE™

Selection of our books indexed in the Book Citation Index in Web of Science™ Core Collection (BKCI)

Interested in publishing with us?
Contact book.department@intechopen.com

Numbers displayed above are based on latest data collected.
For more information visit www.intechopen.com

7

Application of Microseismic Monitoring Technique in Hydroelectric Projects

Nuwen Xu, Chun'an Tang, Hong Li and Zhengzhao Liang
Institute of Rock Instability and Seismicity Research,
Dalian University of Technology,
People's Republic of China

1. Introduction

Slope instability and landslides have been always one of the most significant subjects of slope engineering, and also one of the hottest and most difficult topics in geotechnical engineering research all over the world. How to effectively predict and control slope failure hazards and ensure safety of these engineering projects is a significant task that people often probe. Recently, with the rapid and sustainable development of China' economy, mines proceed to ever greater depth and into more and more complex geological settings. Meanwhile, civil engineering projects, particularly large hydroelectric projects (e.g. West-East power transmission) in southwest China, are being advanced at greater buried-depths. These projects are challenged by violent rock mass failure processes due to deep cracks and faults, high stress levels, loose rockmass with low wave velocity, intense weathering, inter-layer extrusion zones and unloading fissures etc. As we know, extensive use of measurement technology, such as GPS (Global Positioning System), SAR (Synthetic Aperture Radar) Interferometry, TDR (Time Domain Reflectometer), multiple position extensometers, convergence meters and surface subsidence monitoring, is currently found to be very useful in surface deformation monitoring of slopes. However, it is unrealistic for them to effectively monitor the occurrence of micro-fractures in deep rock masses prior to the formation of a macroscopic rock fracture outside slope surface. With regard to rock slope, these internal micro-fractures may often lead to macroscopic instability of slope. Consequently, there must be an intrinsical correlation between rock slope macro-instability and its internal micro-fractures (i.e., microseismicity). It is well known that rocks loaded in testing machine and rockmasses that are stressed near underground excavations emit detectable acoustic or seismic signals. If these signals can be captured sufficiently clearly as seismograms by a number of sensors nearby, the origin time of seismic events, its location, another source parameter such as source radius, static stress drop, dynamic stress drop and apparent stress can be estimated (Cai and Kaiser, 2005; Mendecki, 1997). Microseismic monitoring techniques have been thus employed to locate damage in order to identify and delineate the potential hazardous regions in rock engineering practice, which would provide early warning of rock slope instability.

Earthquakes with local magnitude lower than 2.5 are called microearthquakes and are rarely felt. Microseismicity may be induced in mining areas, hydroelectric reservoirs or geothermal sites. Those activities involve changes in stress, pore pressure, volume and load, which can

result in sudden shear failure in the subsurface, usually along pre-existing weakness zones such as fault structures. Therefore, long-term microseismic monitoring in related fields above would have a potential to reveal fracture geometry and to investigate the progressive failure of rock masses. During the past two decades, microseismic monitoring technique has been emerged from a pure research means to a mainstream industrial tool for daily safety monitoring at various geotechnical engineering. Plenty of engineering applications of microseismic monitoring technique were carried out in South Africa, Canada, Japan, Australia and North America. Significant achievements have been obtained in open pit slopes (Abdul-Wahed et al., 2006; Lynch et al., 2005), underground mining (Ge, 2005; Hudyma, 2008; Kaiser, 2005; Mendecki, 2000), tunnels (Hirata et al., 2007; Milev et al., 2001), oil and gas exploration and development, and electricity generation by hot dry rock (Tezuka and Niitsuma, 2000) etc. The application and its related theory of microseismic monitoring technique have been also investigated in China. For instance, in order to real-time monitor and analyze microseismicity of the left bank slope at Jinping I Hydropower Station, along Yalong River in Sichuan province, a routine micro-seismic monitoring system was installed in May 2009 and the monitoring results can identify and delineate the potential rock damage regions and sliding surface (Xu et al., 2011c; Xu et al., 2010). Some researchers (Jiang et al., 2006) have studied the relationship between strata fracturing and rock-burst in underground mines and discussed the possibility of forecasting rock-burst based on the rules of strata fracturing monitoring by different microseismic monitoring systems. In order to study the progressive failure of geological structures (faults, karst collapse colums) and predict their microseismic activities associated with water inrush, micro-seismic monitoring was employed in deep mines successfully (Jiang et al., 2006). Tang et al. (Tang et al., 2011.) investigated the tempo-spatial distribution of microseismicity for rockburst prediction of the drainage tunnels with a maximum buried depth of 2 500 m in Jinping II Hydropower Station, which is also situated in Sichuan province, southwestern China. These achievements play a significant role in solving the problems of mine field stress, slope instability, hydro fracturing as well as rockburst hazards, and promote the application and development of microseismic monitoring technique worldwide.

This chapter attempts to first of all give a brief introduction of microseismic monitoring technique, including the basic principle, the development history, constitution, positioning methods and waveform identification. Then engineering application of microseismic monitoring technique have been investigated through three typical hydroelectric projects such as Jinping I hydropower station, Dagangshan hydropower station and Jinping II hydropower sation in southwest of China. By analyzing the excavation-induced microseismicity, it is possible to identify and delineate the particular failure regions that underlie the seismic activity in order to perform early warning and advance support measures in rock slopes and tunnels. Meanwhile, tempo-spatial distribution of seismic source locations during construction and impoundment of dams can be used to determine the existence of micro-fractures associated with buildup, stress shadow and stress transfer in deep rockmass of rock slopes.

2. Microseismic monitoring technique

2.1 The basic principle

It is well known that rocks loaded in testing machines and rock masses that are stressed near underground excavations or inside the rock slope emit detectable acoustic or seismic

signals, and seismic monitoring techniques have been developed as powerful methods for remotely determining the integrity of the rock mass in rock engineering practice (see Fig.1). This technique can be used to provide information on location, extent, and mechanism of any damage processes occurring in the rock mass. By incorporating source location and source parameter estimates, it is now possible to visualize the development of microseismic events in 3D space (Cai and Kaiser, 2005). Compared with traditional measure technology, microseismic monitoring is a remote, three-dimensional, and real-time monitoring technique. Moreover, further analysis of the scale and characteristics of rock failure can be performed according to hypocenter parameters recorded by the system. Having recorded and processed a number of seismic events within a given volume of interest over time, one can then quantify the changes in the strain and stress regimes and in the rheological properties of the rock mass deformation associated with the microseismicity (Trifu and Shumila, 2010). This in turn allows estimation of quantities like rock mass stability over space and time, and thereby prediction of slope failure precursor or rockburst of deep-buried tunnels.

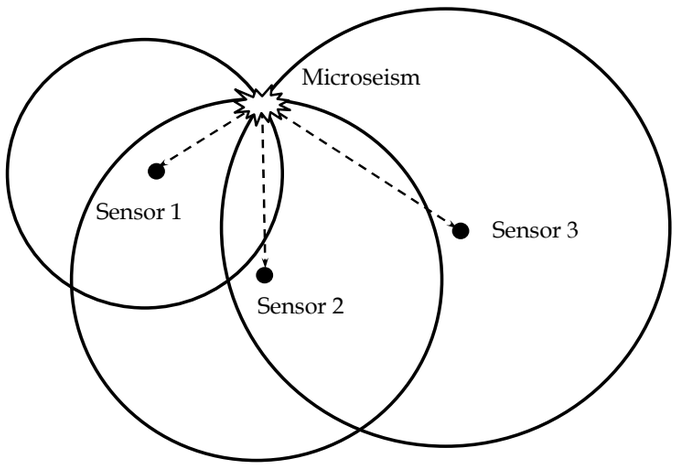

Fig. 1. Sketch diagram of the principle of microseismic monitoring.

2.2 The development history

The monitoring of microseismicity can be dated from 1908 when the first earthquake observation station was installed at Bochhum mine in Ruhr, Germany. The application of monitoring the signals of elastic wave induced by rock mass fractures in underground mines can be traced back to 1942 (Potvin and Hudyma, 2001). However, the significant achievement of seismic monitoring in understanding and investigating mine earthquakes became reality until extensive seismic sensors monitoring network was installed at Erpm mine in South Africa on 1960s (Cook, 1964). The manufacture and monitoring researches of mine seismic monitoring system have been highly paid attention to and rapidly developed when mine seismic monitoring was regards as significant approach of monitoring and prediction of mine rockburst and instability. Nowadays, the mine structures and three dimensional visualization seismic data can be integrated to provide a valid monitoring tool for investigating seismicity and excavation-induced effect in mining, petroleum, and hydropower fields (Kaiser, 2005; Lynch and Mendecki, 2001).

Currently, there are several typical microseismic monitoring systems all over the world such as ISS in South Africa, ESG in Canada, SOS in Poland and ASC in England. ISS systems were popularly used in mines and open pit slopes (Lynch et al., 2005). ESG systems have an extensive application in Canada, Australia and China (Urbancic and Trifu, 2000; Xu et al., 2011c). SOS and ASC systems are also adopted in some projects worldwide. In China, the beginning of studying microseismic monitoring was a little late, and there were few engineering applications in the early stage. Nevertheless, with decades of continuous development, there are some achievements in equipment manufactures and software designing of microseismic monitoring in recent years. Currently, the popular seismic monitoring systems above were imported to further-investigate rockburst in mines and deep buried tunnel, failure mechanism in rock mechanic and rock engineering in China. The technique develops continuously with the rapid progress of computer and data acquisition technology. In brief, it can provide a new approach to investigate spatial rupture pattern of overburden and excavating-induced stress distribution in mines, tunnels and rock slopes.

2.3 The constitution of microseismic monitoring system

It is worth noting that the microseismic monitoring systems adopted in the present study are manufactured by the Engineering Seismology Group (ESG) in Canada, although the wireless transmission system MMS-View was developed by Mechsoft Co. Ltd. in China to be supplemented into the monitoring system. The seismic monitoring network consists of Hyperion digital signal processing system, Paladin digital signal acquisition system, a number of uniaxial/triaxial acceleration transducers deployed in boreholes drilled from rock mass in rock slopes or tunnels, and the 3-D visualization system namely MMS-View based on remote wireless transmission (see Fig.2). Accelerometers are connected to the

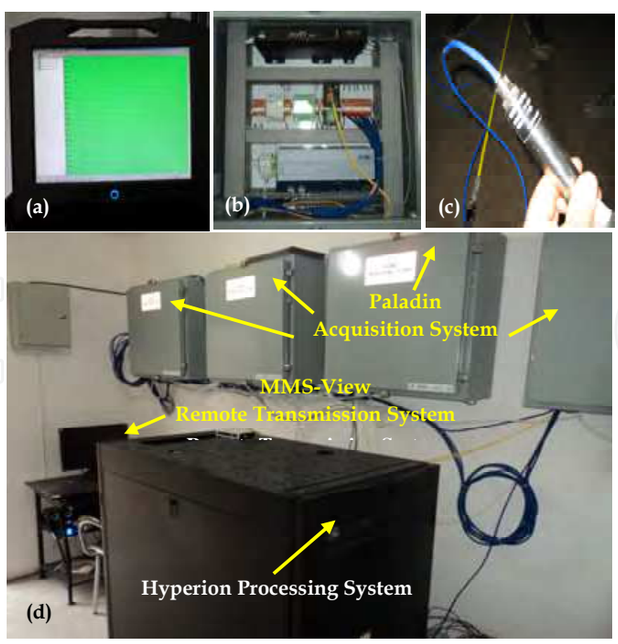

Fig. 2. Constitution of microseismic monitoring system: (a) Hyperion digital signal processing system, (b) Paladin digital signal acquisition system, (c) acceleration transducer, and (d) the center of the site monitoring system.

substations (namely Paladins acquisition system) using copper twisted-pair cables. The substations are connected in series to the central system (namely Hyperion processing system) using optical fiber cables and network cables. Paladin units rely on a pulse per second (PPS) signal originated from the Paladin Timing Source over the network. This can allow the data from each Paladin to be accurately time-stamped, ensuring that multiple units are in synchronization (Urbancic and Trifu, 2000). Finally, the seismic data recorded are transmitted from the on-site center to the office by GPRS for further analysis. The three systems are fully described in (Tang et al., 2011.; Xu et al., 2011a; Xu et al., 2011c; Xu et al., 2010). The processing system in the central station digitizes the data with a sampling frequency of 10 kHz and performs preliminary event detection when the recorded signals of the substations exceed a given threshold, using the Short Time Average vs Long Time Average algorithm (STA/LTA). The system then calculates in real time a preliminary hypocenter determination with a homogeneous velocity model and records the data on hard disk. This detailed specification can be found in (Trifu and Shumila, 2010; Xu et al., 2011b; Xu et al., 2010).

2.4 Positioning accuracy and waveforms identification

In practice, artificial fixed position blasting tests are usually adopted to calculate the mean wave velocity. Moreover, the typical waveforms such as blasting signal, micro-fracture of rock mass, tap-test signal and background noise etc. are also identified and distinguished. Herein, the blasting tests for wave configuration in Dagangshan project is taken as an example (Xu et al., 2011b).

2.4.1 Wave velocity testing

The wave velocity influences the first break time that elastic wave arrives to sensors. Therefore, wave velocity configured in the monitoring system has a great influence on seismic source location. In this respect, wave velocity of rock mass within the monitoring scope must be calibrated before testing the positioning error of the system. The mean velocity of elastic wave is first determined as 4500m/s according to wave velocity tests of rock samples on-site in Dagangshan project. Then the wave velocity of blasting tests is calculated inversely and adjusted through data analysis program. The waveform of the first blast test recorded is shown as Fig. 3, which occurred inside the drainage tunnel of the dam foundation at 1081m level on 04:25:41, May 7, 2010. The testing results show that the mean velocity of P wave and S wave are 4400m/s and 2540m/s respectively in the scope of monitoring, which coincide with testing results of wave velocities on-site. The wave velocities can be then used to locate seismic events.

After calibration of wave velocity inside rock mass in the scope of monitoring, three localization tests using artificial blasts method were performed in order to check positioning accuracy of the seismic monitoring installation at the right bank slope. The coordinates of three artificial blasting tests location and their positioning recorded by the monitoring system are shown as Table.1. The results of blasting tests show that microseismic source location error is less than 10 m in the scope of the sensor array. This validates that the accuracy of the microseismic monitoring system installed at the right bank rock slope is high. Fig.4 shows the spatial comparison between an artificial blast test location and its positioning result recorded by the system.

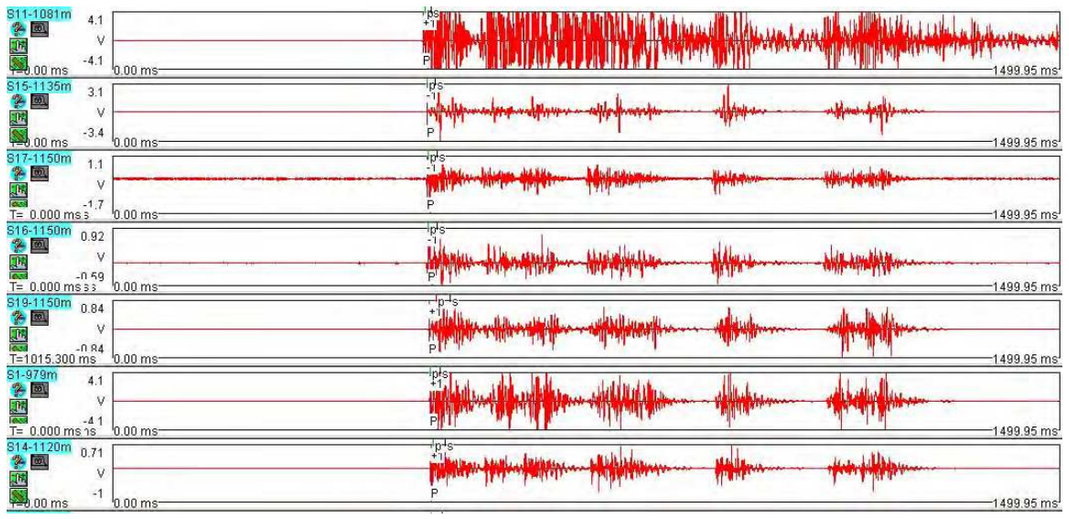

Fig. 3. Waveform of the first artificial blast recorded by the system.

No	Blast date	Blast time	Height /m	Blast test coordinates/m			Locating coordinates/m			Error/m			Absolute error/m
				X	*Y*	*Z*	*X*	*Y*	*Z*	*X*	*Y*	*Z*	
1	05-07	04:25:41	1081	520837.2	3259177.8	1082.7	520835.2	3259181.7	1074.5	2.0	3.9	8.2	9.3
2	05-07	19:08:52	1081	520829.4	3259169.8	1082.8	520823.9	3259173.5	1080.8	5.5	3.7	2.0	6.9
3	05-09	20:47:39	1081	520823.5	3259172.3	1082.8	520826.6	3259179.9	1084.3	3.0	7.6	1.5	8.3

Table 1. Comparison of coordinates of artificial blasting with those of microseismic monitoring localization (in 2010).

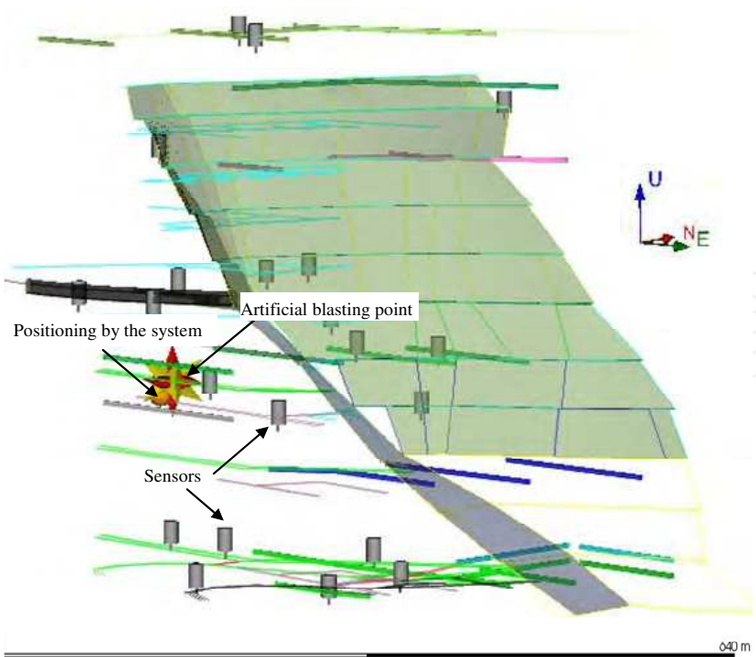

Fig. 4. Spatial comparison between one artificial blasting location and its positioning result recorded by the system.

2.4.2 Waveform identification and analysis

Through field observation and investigation, the preliminary events recorded by the microseismic monitoring system at the right bank slope are classified into three main types: rock micro-fracture events, excavation blasting events, vibration and noisy events (Xu et al., 2010). Fig.5 shows the typical waveform of microseismic event. It can be observed that such waveforms are very smooth with amplitude range from dozens of mV to hundreds of mV, magnitude distribution nearby -1.2, and energy release around about 102 Joule. The waveform of blasting tests is shown above in Fig.3. The sensor No.11 (S11-1081m), which was close to the shot point, picked up the elastic wave induced by blasting tests at first. The

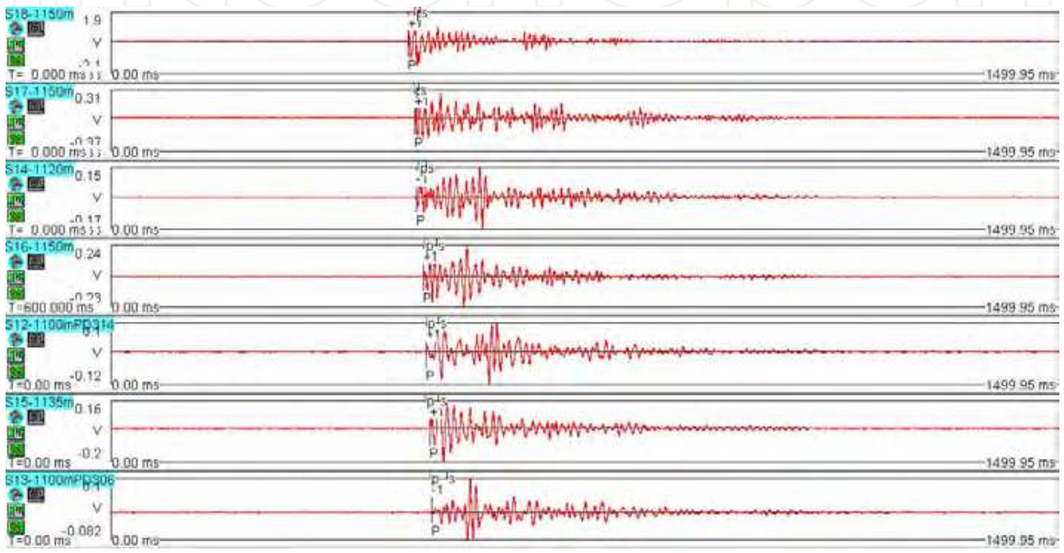

Fig. 5. Waveform of a typical microseimic event.

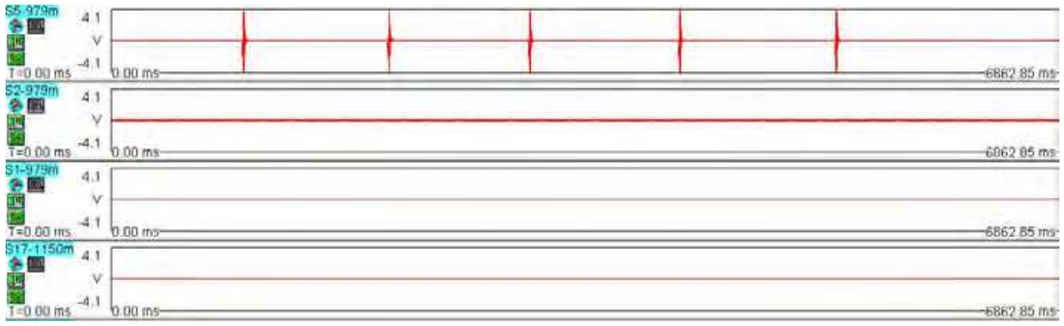

(a)

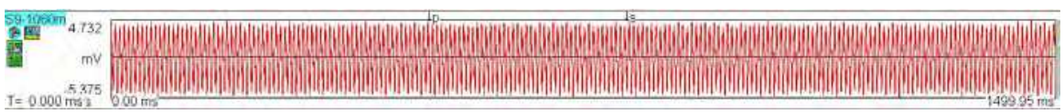

(b)

Fig. 6. Waveforms of vibration and noise: (a) Waveform of tap tests, and (b) Waveform of electricity interference.

amplitude of the blasting event was about 4.1V and the moment magnitude was -0.91. Fig.6 shows the waveforms of different machinery vibration and noise. The characteristics of such waveforms are repeat shaking along time shaft and stripped. In order to verify the installation accuracy of the sensors, artificial tap tests corresponding to each sensor are performed as shown in Fig.6 (a). It can be seen that the amplitude of sensor No.5 (S5-979m) in acquisition interface is greatly higher than other sensors when knocking rock mass nearby the sensor No.5 at 979m level. The results demonstrate that the coordinates for each sensor input into the system are correct.

3. Engineering application

3.1 Stability evaluation of the left bank slope of Jinping I hydropower station

3.1.1 Project background

Jinping I hydropower station is located at the sharp bend of Jinping on the middle reach of Yalongjiang River, near Xichang, about 500 km southwest of Chengdu, Sichuan province, China. It is situated within the aslope transition zone from the Qinghai-Tibet Plateau to the Sichuan Basin. The project has a double-curvature arch dam with a maximum height of 305 m and a total installed capacity of 3300 MW, which will be the highest arch dam in the world nowadays. The geological structure of this area is complex due to the great variability in lithology and lithofacies, intensive tectonic deformation and folding, abundant fractures, and widespread metamorphic terranes. Complex geological conditions greatly affect the engineering design in the project (Qi et al., 2004; Zhong et al., 2006). As illustrated in Fig.7 (a), the dam site is located in a reach 1.5 km between Pusiluo gulley and Shoupa gulley. The natural slopes and the left slope after excavation are shown in Fig.7.

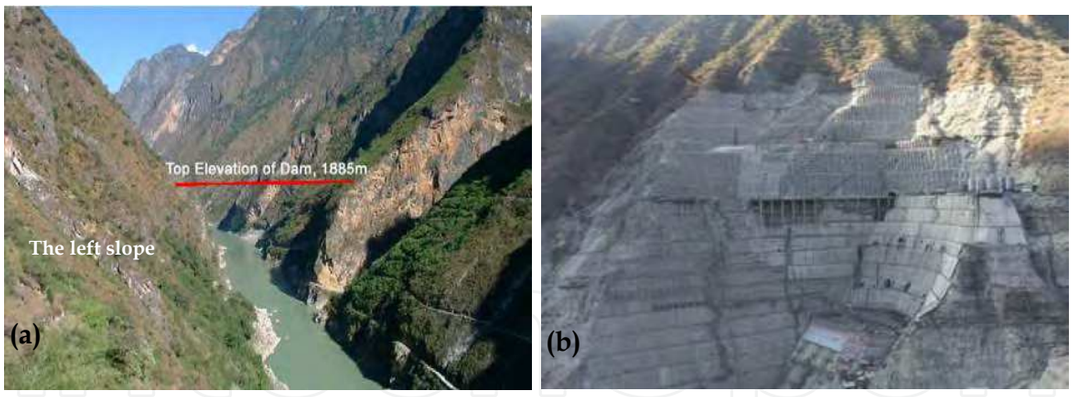

Fig. 7. Geomorphic photograph of dam site: (a) before excavation (Zhong et al., 2006); (b) the left slope after excavation.

The left bank slope of the hydropower station has lots of prominent characteristics such as large scale, complex engineering and technical conditions, high and steep natural valley slopes, higher stress levels, a strong rock unloading, inter-layer extrusion zones and deep cracks in the complex geological site. The behavior of such features plays a critical role in the stability evaluation, especially in the processes of excavation of the slopes and different tunnels. Furthermore, plenty of deep cracks and faults such as F_{42}, F_5, F_8 and lamprophyres (X) form huge latent instable blocks in these areas. The instable blocks will induce the potential instability of the slope.

3.1.2 Tempo-spatial distribution of microseismicity

Although lots of researches on microseismic monitoring have been carried out, little work was found to investigate slope stability of large-scale water conservancy projects, especially high rock slopes. Our surveys present here highlighted the continuous characteristics of microseismicity induced by continuous excavation and grouting inside the rockmass in the left bank slope. After filtering out the noisy events, a dataset of 1521 seismic events with M_w -2.5 to 0.2 occurred from June 2009 to May 2011. Fig.8 shows the temporal distribution of seismic source locations. It can be observed that the daily rate of events ranges from 1 to 14 with small bursts of activity every 3-5 days. Most of the seismic events are recorded during several swarms. According to on-site observation and analysis, such swarms are partly caused by stress redistribution of deep rock mass inside the left bank slope on the basis of continuous excavation in different tunnels or at the bottom of the rock slope, and partly caused by a secondary extension of deep rock mass fissures due to high-pressure grouting. A notable phenomenon that the frequency of the recorded microseismic events increases drastically right after excavation and grouting is obtained. In addition, there is no microseismic signal during the period from 1 December to 17 December 2009. The reason is that the seismic monitoring network broken down caused by perturbation of large machinery on-site. Seismic source locations decrease sharply after the main excavation of rock slope stopped and the pouring of dam began in October 2009 (see Fig.8).

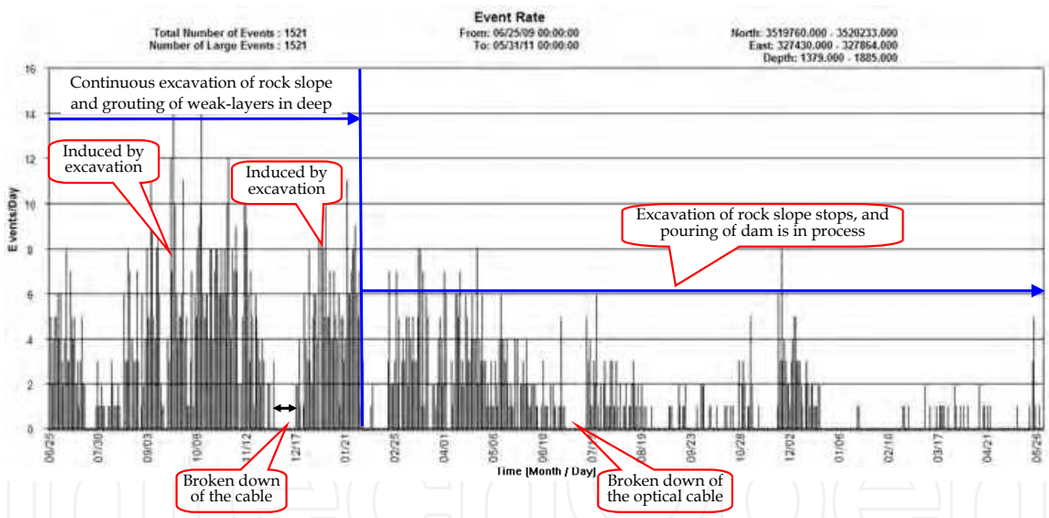

Fig. 8. Temporal distribution of seismic source locations.

The spatial distribution of the seismic source locations recorded is presented in Fig.9. The figure can highlight the distribution and migration characteristics of micro-fractures clusters in deep rock mass of the left slope. Fig.9 (a) shows that majority of microseismic events predominantly occurred along the slope of the dam spandrel, especially along the faults f_5, f_8 and X. To further emphasize the relationship between the geological structures and spatial distribution of seismic source, Fig.9 (b) displays the microseismic events in an aerial view. It can be found that seismic source clusters are concentrated at the bottom of the downstream slope nearby the dam, which implicates that the design and implementation of the sensor array meet the need of global monitoring of the interest areas at the left slope. Discarding extreme values out of the study volume, it is apparent that the regions characterized by

seismic clusters show strong correlation with pre-existing geological structures, especially faults or fractures inside the rock slope (Shumila and Trifu, 2009).

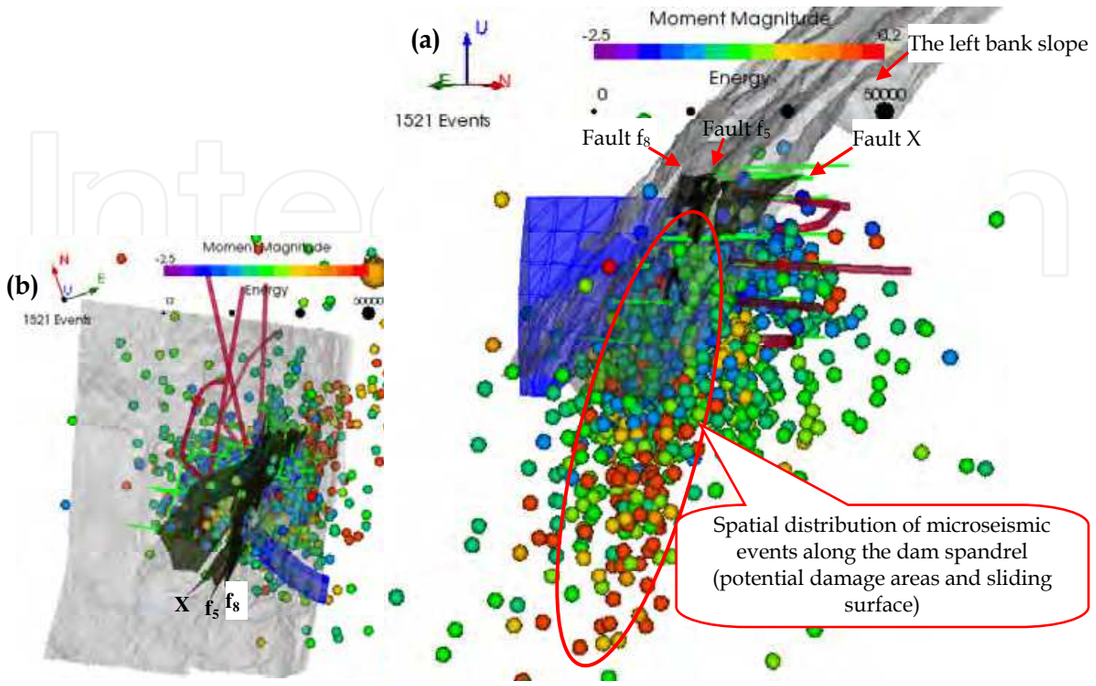

Fig. 9. (a) Cross-section looking east-north projection of the microseismic events recorded between June 25, 2009 and May 31, 2011. (b) Aerial view of the monitoring area is shown to illustrate the relationship between source locations and topography (the spheres present microseismic events, the size presents moment magnitude. The bigger the sphere is, the higher the moment magnitude is, and vice versa).

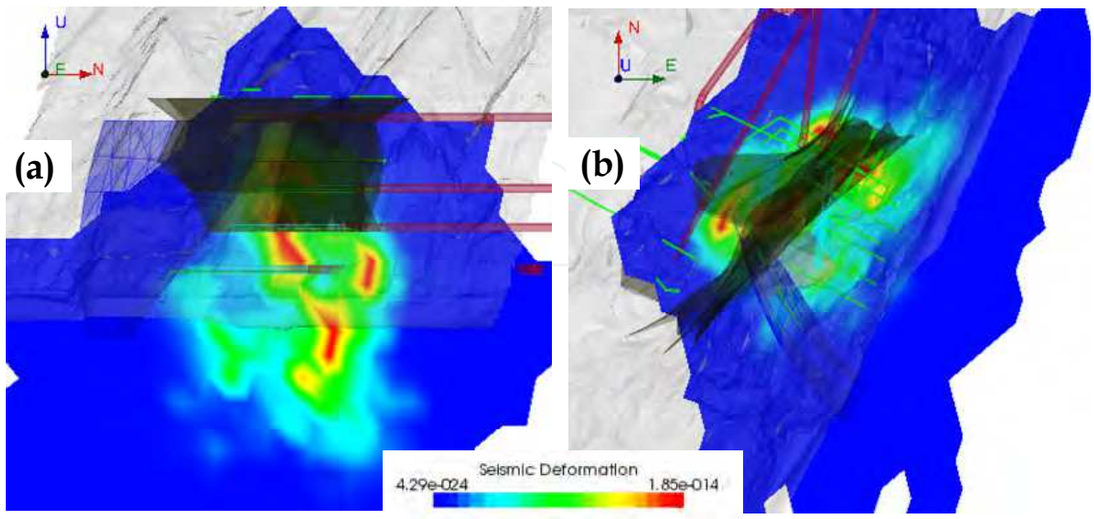

Fig. 10. Seismic deformation contours in (a) south-north vertical cross-section looking east and (b) north-easting plane at 1730m elevation looking down. Different colors represent various quantities of seismic deformation per unit volume.

Evaluating the seismic deformation is important for the understanding of stress redistribution and geomechanical processing taking place on site (Shumila and Trifu, 2009). As is shown in Fig. 10, the seismic deformation tends to be related to pre-existing geological structures such as faults f_5, f_8 and X, as well as to the excavation of tunnels inside the left slope. It can be seen from Fig.10 (b) that the maximal seismic deformation is mainly located along the faults mentioned above, and focused at the regions of elevations between 1670m and 1829m (Fig.10 (a)). Worth noting, the value of the seismic deformation is very small, which reveals that the left slope can be estimated as a stable slope currently. As expected, the seismic deformation is very prominent in the areas of pre-existing faults and man-made structures.Spatial distribution regularity of microseismic activity and seismic deformation maps can be used for two aspects: (1) support selection and tracking of rock mass condition for excavation support rehabilitation in the left slope; and (2) future routine monitoring plan and corresponding equipments rearrangement on the hazardous areas, especially after impoundment of the dam which will induce stress redistribution of deep rock mass inside the slope.

3.1.3 Comparison study between seismic monitoring and field observation

The correlation between microseismicity and excavation-induced faults and cracks are illustrated in Fig.11. The microseismic events mainly occur at the potential sliding surface, nearly 90 m away from the surface of the rock slope. It can be seen from Fig.11 (a) that microseismic events with large magnitude and high energy mainly focus at the bottom of the downstream slope. Such events are caused by the foundation pit excavation of the dam according to field observation. Conversely, microseismic events with small magnitude and low energy almost concentrate along the weak structures such as the pre-existing faults and some tunnels in the excavation phase. It is worth noting that not all geological structures are directly observed and mapped. Therefore, it is the occurrence of microseismicity that characterizes if an unknown geological structure is active. Microseismicity related to these structures is also evidence of rock mass degradation from elevated stresses as each microseismic event indicates rock fracturing (Trifu and Shumila, 2010).

Combining with on-site observation and analysis of microseism swarms, there is a direct correlation with some identified geological structure (e.g., faults f_5, f_8 and X) and newly identified geological structure. Region (I) in Fig.11 (a) shows that microseismic events are mainly located along the pre-existing faults such as f_5, f_8 and X. This can be interpreted as tensile failure subject to excavation of the dam foundation and it has an active zone along the dam abutment range from 1670 m level to 1829 m level. Region (II) in Fig.11 (a) can be interpreted as pressure-shear failure that is responsible for seismic events of large magnitude recorded at the bottom of the slope (see Fig.11 (b)) and it has an active area of about 150 m in diameter; Region (III) in Fig.11 (a) can be demonstrated that it is activated by local stress perturbations due to excavation of the corridor in the downstream slope at 1730m level (Fig.11(c)). Therefore, microseismicity in the left slope occurs due to the day to day tunnels excavation activity and grouting to the weak-layers in deep rock mass, and have typically been the result of most cracks in tunnel sidewalls and at the bottom of the slope. As such, the microseismic monitoring system implemented at the left bank slope can identify, locate and quantify microseismicity and potential damaged areas, allowing for a better understanding of the deep rock mass fracture mechanism. They then contribute to the management and mitigation of seismic hazards, for improving the rock slope stability and enhancing the capability of risk forecasting.

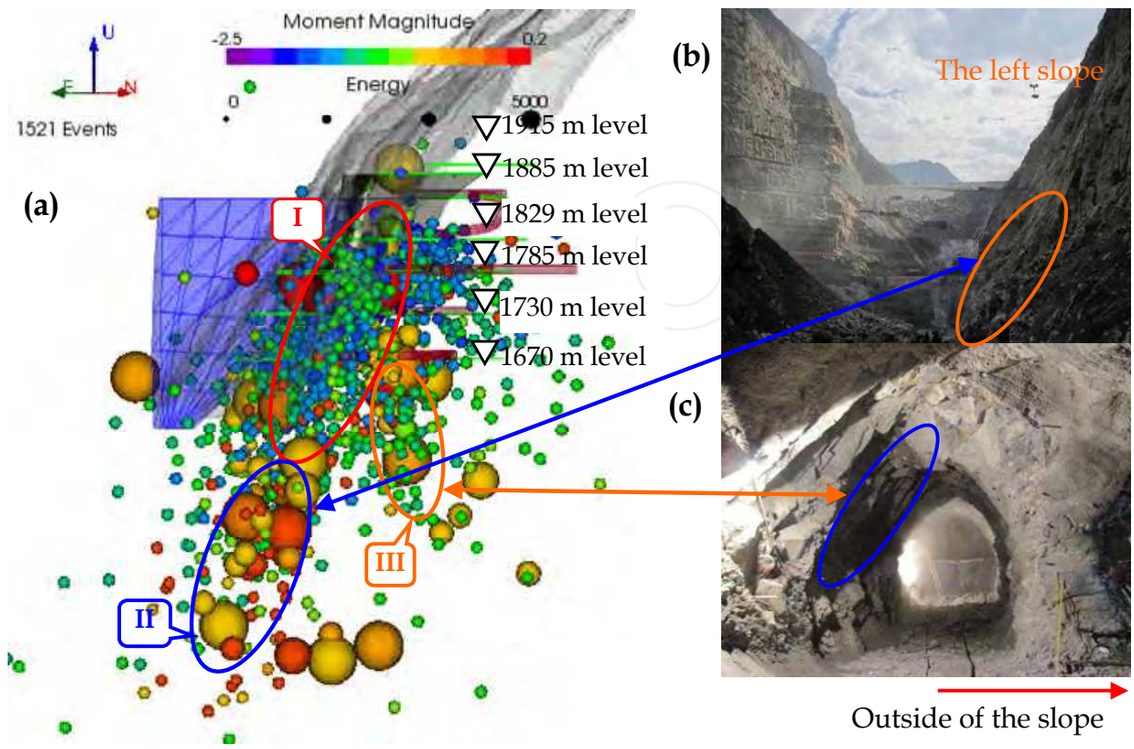

Fig. 11. Correlation between spatial distribution of microseismic events clusters and field observation: (a) Spatial distribution of source location; (b) Fractures at the foundation pit; (c) Cracks at the sidewall of the drainage tunnel on 1670 m level.

3.2 Excavation-induced microseismicity at the right bank slope of Dagangshan hydropower station

3.2.1 Project background

Dagangshan Hydropower Station is located at Dadu River in Sichuan province, south-western China. The project is one of the large scale hydroelectric constructions which are currently exploited along the mainstream of Dadu River. It has a double-curvature dam with a maximum height of 210 m, and a total installed capacity of 2, 600 MW. Complex geological conditions greatly affect the engineering design and construction in the project. The layout of key water control and the right bank slope after excavation are presented in Fig.12 (a) and (b), respectively. The right bank slope of the project has complicated geological conditions such as faults, dykes, unloading cracks zones and joints with cracks development. In particular, faults X316-1 and f_{231} are the most significant factor that influences the stability of the rock slope. Weathering and unloading of rock mass inside the slope are also very serious. Plenty of investigations and excavations reveal that deformation failures have superficially occurred on the slope due to stress rearrangement as a result of sapping of the River. A microseismic monitoring system was adopted to further analyze the right bank slope stability in June, 2010. The spatial arrangement diagram of sensors at eleven elevations is shown in Fig.13.

Fig. 12. Geomorphic photograph of the dam site: (a) The layout of key water control, and (b) The right bank slope after excavation.

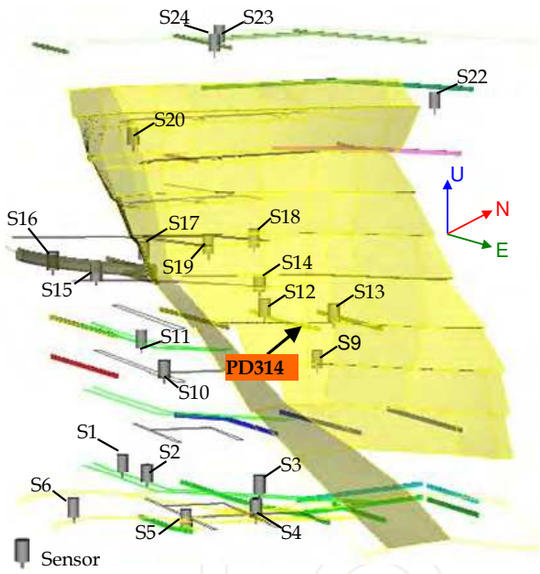

Fig. 13. Spatial arrangement diagram of sensors at eleven elevations.(Noting that three sensors No.7, 8, 21 to be installed later on due to the limitation of tunnel condition. The different color columns present different tunnels such as transportation tunnels, drainage tunnels, and exploratory headings).

3.2.2 Tempo-spatial distribution of seismic events

After filtering out the noisy events, a dataset of 420 seismic events was recorded within a given volume of interest over time from May 12 to October 20, 2010. Forty-eight percent of the data base such as blasting events, mechanical vibration and background noise events was rejected. A plot of cumulative number of seismic events recorded from the selected time shows one period of increased micro-seismic activity: July 20 to August 5, 2010. This graph is compared with the time history of excavated rock mass at the bottom of the rock slope as shown in Fig.14. It can be observed that the curve of cumulative seismic events in Fig.14 (a)

goes with almost the same tendency as the curve of excavated volume of rockmass (volume blasted) in Fig.14 (b) does. This is a good correlation which illustrates a clear consistency between the volume of rock mass being excavated and the total number of seismic events. Therefore, it can be noted that excavation activities play a great role on the levels of extension fracturing within a rock slope. Seismic data recorded here confirm this link, and go further by providing routine micro-seismic monitoring to quantify the effects that excavation is having on the slope. Additionally, it can be seen from Fig.14 (a) that the daily rate of seismic event ranges from 1 to 7 with small bursts of activity per 5-7 days. The mean rate of events during the selected period is 3 per day. According to on-site investigation, swarms of micro-seismic events are caused by excavation-induced stress redistribution of deep rock mass inside the right bank slope.

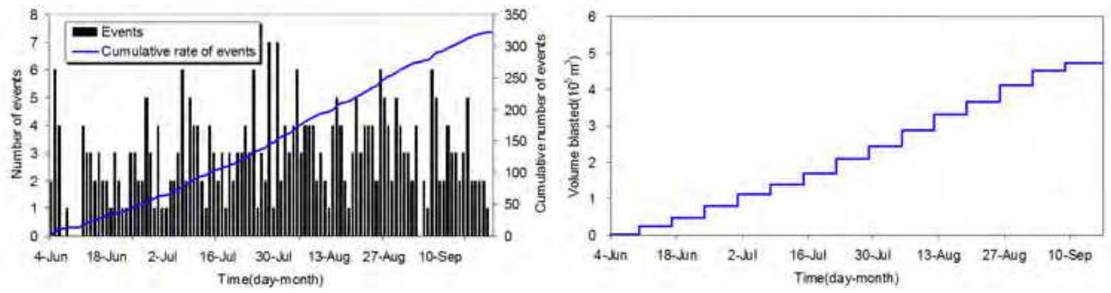

(a) (b)

Fig. 14. (a) Graph of the cumulative number of seismic events, and (b) the curve of cumulative amount of rockmass removed from the right bank slope in chronological order. The general forms of the two graphs are similar (in 2010).

The spatial distribution of the events recorded during the selected period is shown in Fig.15. Fig.15 (a) shows the absolute locations of all events including micro-seismic events, production blasts and some noises without manual processing. Fig.15 (b) shows the micro-seismic events recorded after eliminating interference events. During this period of micro-seismic monitoring, the rock slope was excavated continuously from the elevation 1070m to 980m and shearing-resistance tunnels at 1120m and 1150m elevation were also excavated, respectively. The micro-seismic event locations show that hypocenters are concentrated on these excavation zones, and this concentration is due to the excavation configuration. It can be seen from Fig.15 that hypocenters follow the working faces and they are located where the excavation is carried out, making it possible to correlate them unambiguously with the construction areas (Abdul-Wahed et al., 2006). Therefore, the regions inside the right bank slope, where micro-seismicity is active or inactive, can be identified and delineated.

In addition, Fig.15 (b) shows the majority of micro-seismic events predominantly occurred around the elevation 1180m of the upstream slope, especially focusing on the hanging wall of the fault XL316-1 (Fig.15 (c)). The top view in Fig.15 (c), looking from the upside, shows that the seismic events are being recorded at significant depths into the slope. However, there are small number of seismic events occurred at the toe of the rock slope. This may be partly attributed to residual movements (e.g., unloading crack zones, developed dikes and faults etc.) inside the rock slope at high elevations and/or the excavation of shear-resistance tunnels. On the other hand, it may be also partly due to high stress concentration at the slope toe because of slope geometry. It is known that seismic activity depends on stresses and tectonic conditions, herein the tectonic stress is probably less important in this zone and

the compression stress (normal stress) is higher and helps to reduce the fracturing and the seismic emission (Xu et al., 2011a).

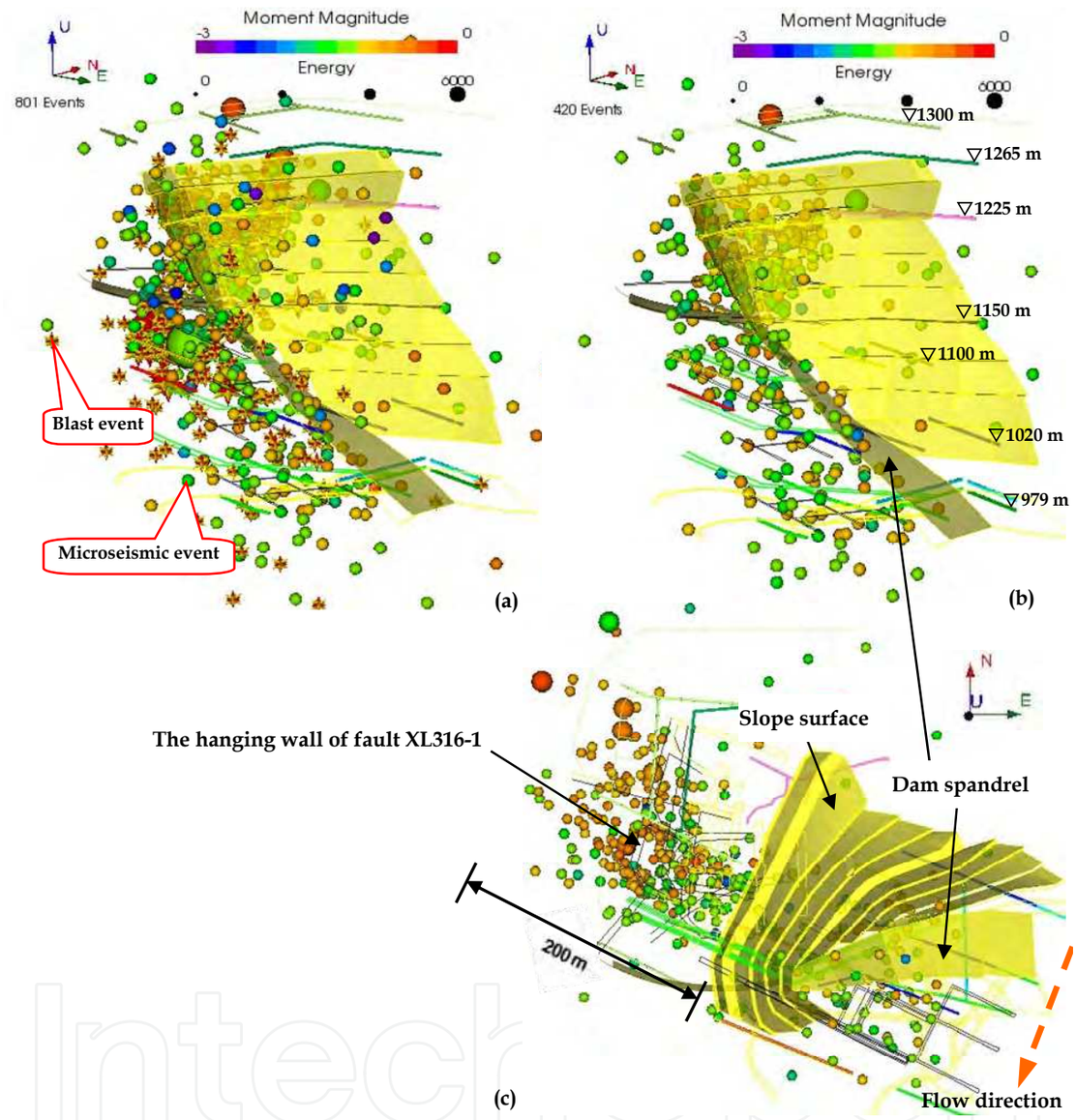

Fig. 15. Spatial distribution of events: all events without processing (a) and micro-seismic events (b), (c). Of which (c) shows top view from the upside, of seismic events recorded from May 12 to October 20, 2010. It is evident that micro-seismicity is being recorded at significant depths here (the spheres denote microseismic events, the size presents moment magnitude. The bigger the sphere is, the higher the moment magnitude is, and vice versa).

3.2.3 Excavation-induced microseismicity analysis

Fig.16 shows the area map of energy loss density induced by micro-seismicity of the rock slope since the operation of the seismic monitoring system. It can be observed that energy loss of the seismic events induced by excavation is mostly concentrated above the elevation

1135 m of the right bank slope, with an obvious spatial distribution along faults XL316-1 and f_{231}. A small volume of energy loss by micro-seismicity occurred at the bottom of the slope. However, the magnitude of the energy loss is very small, the potential impact on the rock slope stability needs continuous database of seismic source locations for in-depth investigation. With accumulation of microseismic data recorded and extension of excavation scale below 980m level at the rock slope later on, further researches on these results will be extensively studied through analysis of rock failure cases occurring in the deep rock mass. Moreover, comparison between Fig.15 and Fig.16 shows that seismic events mainly focused on the working zones. For example, seismic source locations are located precisely at, and slightly nearby the workings, meaning that they can unambiguously be correlated with the advance of the rock slope excavation. This comparison showed that most of event clusters are concentrated around the construction areas.

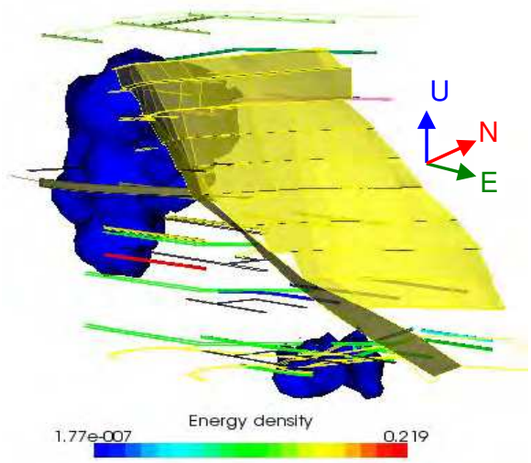

Fig. 16. Density of energy loss induced by micro-seismic events.

3.3 Rockburst prediction of TBM-excavated tunnels in Jinping II hydropower station (Tang et al., 2011)

3.3.1 Project background

Jinping II hydropower station, which is nearby Jinping I hydropower station is located on the Jinping bend of Yalong River at the junction of three counties Muli, Yanyuan, Mianning of Liangshan Yi Autonomous Prefecture, Sichuan Province, China. It takes advantage of the natural elevation drop at the Jinping bend of Yalong River, and water is diverted by a sluice dam to headrace tunnels for power generation. Jinping II Hydropower Station is an important cascade hydropower station on the main stream of Yalong River, with an installed capacity of 4800MW. The Jinping mountain is grand with multiple peaks and cut by deep valleys. The elevations of main peaks are more than 4000 m, with the maximum height of 4488 and the maximum elevation drop of over 3000 m. The project consists of 7 parallel tunnels such as the headrace tunnels No.1 to No.4, the drainage tunnel, the auxiliary tunnels A and B. Among them, headrace tunnels No.1 and No.3 are constructed by TBM tunneling and the diameter is 12.43m. The drainage tunnel is also excavated by TBM with a diameter of 7.2m. The rest tunnels are excavated by drilling and blasting method. The maximum excavated cross sections of headrace tunnels No.2 and No.4 is 13m in dimension

and horseshoe-shaped. Since tunnel construction was commenced, hundreds of rockbursts in various intensities have occurred. Among them, the recent two rockbursts were strong rockburst and very strong rockburst, respectively. The region map of Jinping II hydropower station is shown in Fig.17.

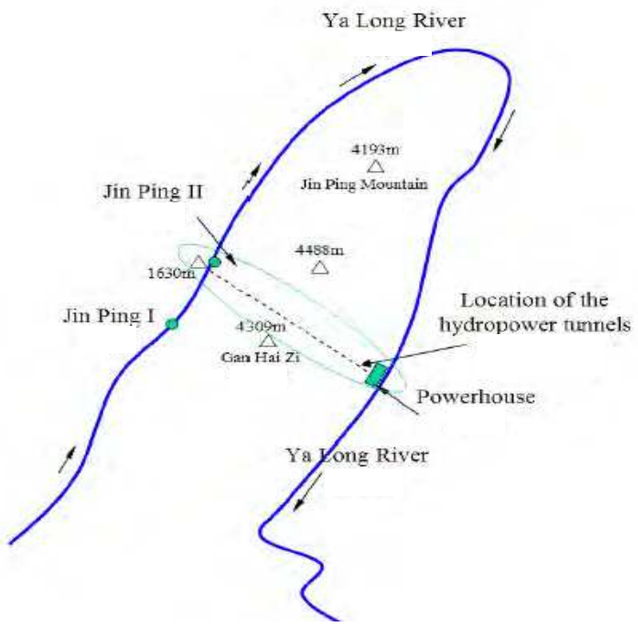

Fig. 17. Regional map of Jinping II hydropower station.

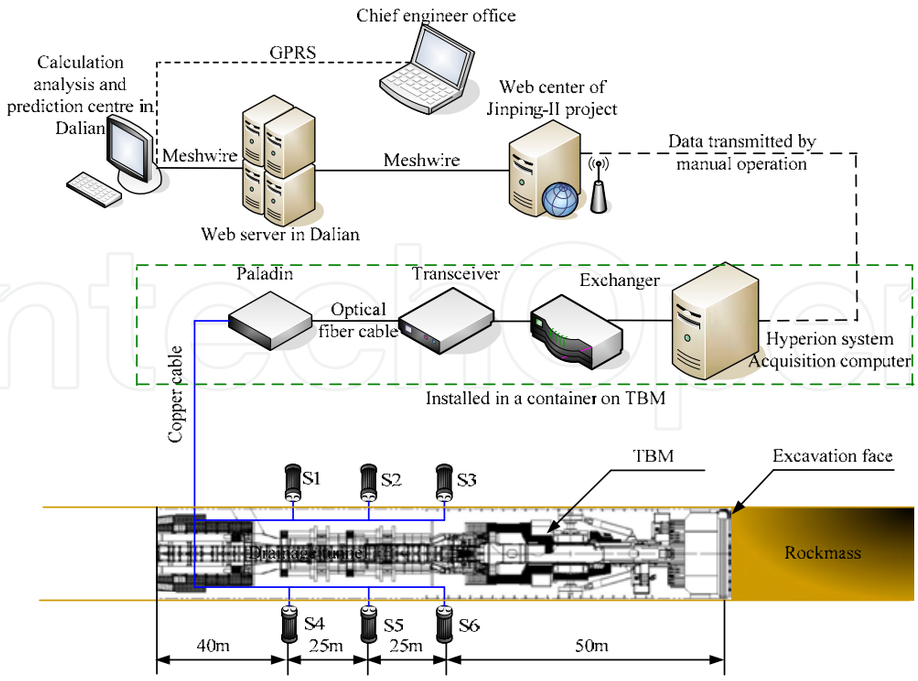

Fig. 18. The monitoring and analysis system for rockbursts during TBM tunneling for Jinping II Hydropower Station.

In September 2009, microseismic monitoring technique was employed into tunnel construction of this project. A movable microseismic monitoring system which can advance with tunneling was established. Six accelerometers were inserted into rock mass of the excavated tunnel to a depth of about 3-4 m. The sensors were placed on bottom of the boreholes. The sensors were placed 30-40 m apart, in three groups each with two sensors in 2 hour and 10 hour direction respectively. The distance between the main tunnel face and the first group of sensors was 30-40 m. The sensors at the tail end moves to the forefront as the excavation of the main tunnel advances. Data were collected continuously by the microseismic data acquisition system and transmitted to a measurement office at a distance of 5-10 km by optical fiber cable. The data were then processed and analyzed. Continuous acquisition and collective analysis of the seismic monitoring data were achieved, which provided an important platform for studies on rockburst monitoring and early warning during TBM tunneling. The microseismic monitoring system is shown in Fig.18.

3.3.2 Tempo-spatial distribution of microseismicity of the strong rockburst on November 28, 2009

The epicenter of a microseismic event may be determined from the difference between the arrival times of the initial microseismic signals at the sensors placed in the borehole. Each circle represents a relative seismic energy. Generally speaking, the everyday safety control at the site of the tunnel excavation can be based on monitoring of microseismic events, calculation of the maximum amplitudes of events measured, and the observation around the rock face. Fig.19 shows the cumulative distribution of microseismic events within 30 days before a strong rockburst in a tunnel of Jinping II Hydropower Station, where the area of concentrated microseismic events is the center of the rockburst.

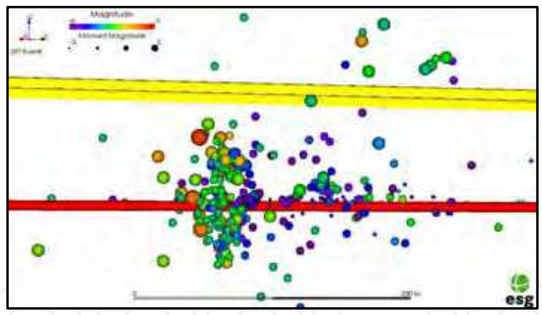

Fig. 19. The cumulative microseismic events within 30 days before the strong rockburst on November 28, 2009.

Fig.20 plots the density nephogram of microseismic events for the strong rockburst on November 28, 2009. Point B was the location of rockburst. The precursors were even more obvious for this rockburst. Anomaly was observed in the nephogram near point B 10 days before the rockburst. The nephogram core was even more evident at point B 2 days before the rockburst. Thereafter, a large-magnitude rockburst occurred, which resulted in extensive tunnel collapse (see Fig.21). Field observation showed that the crater formed by the strong rockburst was 9 m deep and indicated clears signs of structural planes. However, the microseismic location record during the rockburst process shown in Fig.22 suggested that the formation process lasted for 2 minutes, given the crater was as deep as 9 m. With the two minutes from the first microseismic event recorded at 00:42:43 to 00:44:42, about 40

microseismic events were captured by the system. Moreover, most of the seismic events were distributed along a strip, which tallied with the strike of the structural plane identified during field inspection.

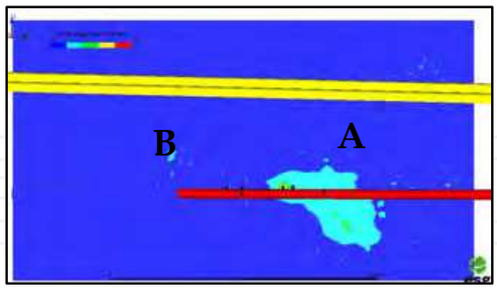

22 days before rockburst

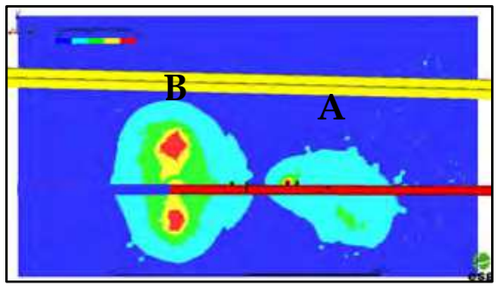

10 days before rockburst

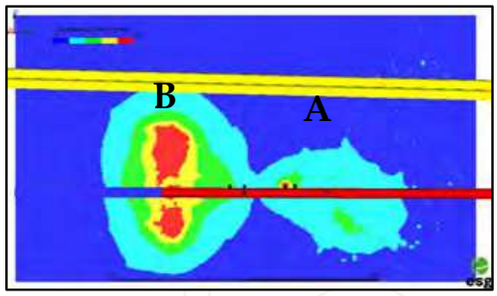

2 days before rockburst

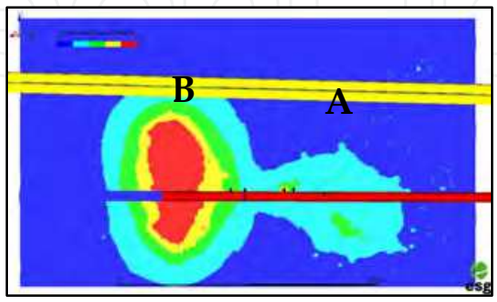

the day of rockburst

Fig. 20. Variation of density nephogram of microseismic events of the strong rockburst on November 28, 2009. (Rockburst occurred in the tunnel section below point B).

Although the prediction of time and magnitude may be very difficult at the moment, the notification of rockburst location may play an important role in mitigating or even prevent rockburst hazards. Fig.23 shows a good example of prevent a rockburst hazard using our MS-based risk-management system. As shown in the first figure in Fig.23, which is the data 8 days before the data shown in the second figure. Based on these figures, we announced a warning of a big possible rockburst in the red color area. After receiving this information, a lot of measure has been done to prevent the occurrence of the rockburst. One of the important actions is the blasting induced energy release within the potential area of rockburst, and the excavation work was successfully executed.

Fig. 21. The damage phenomenon of tunnel and TBM after rockburst on November 28, 2009.

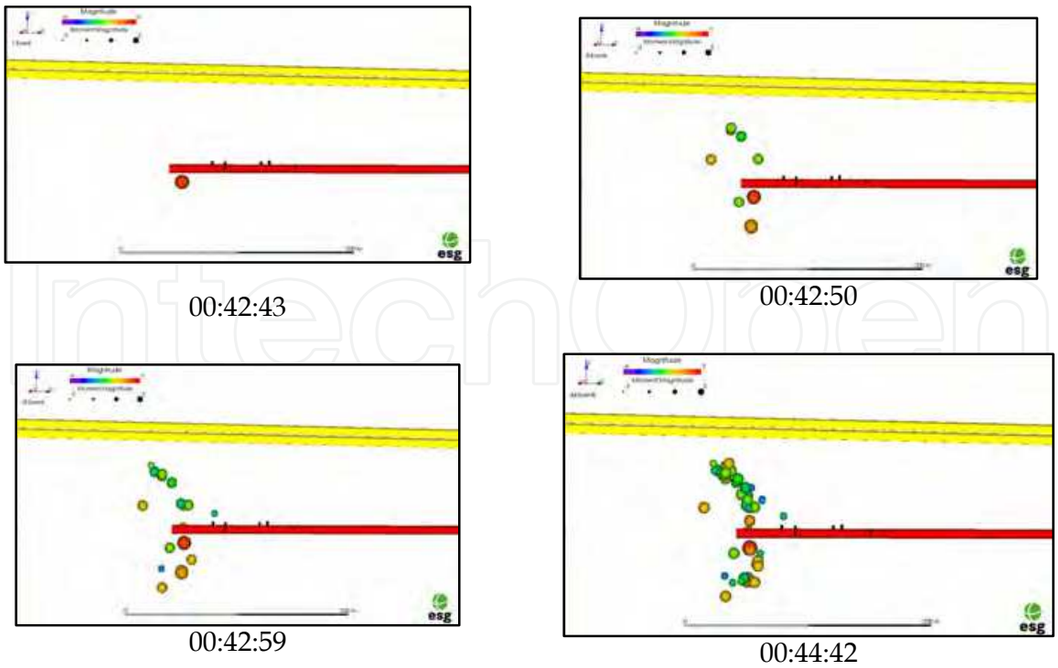

Fig. 22. Seismic source locations record during formation of rockburst crater (The formation of rockburst lasted for 2 minutes).

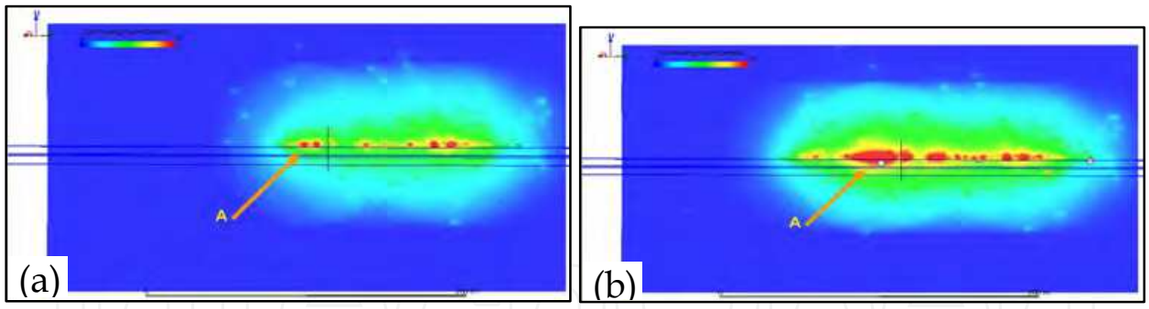

Fig. 23. Variation of density nephogram of microseismic events showing the potential location for rockburst.

4. Conclusions

This chapter focuses on understanding the microseismicity induced by continuous excavation or grouting in high rock slopes and tunnels of three large-scale hydroelectric projects such as Jinping I hydropower station, Dagangshan hydropower station, Jinping II hydropower station. The following conclusions can be drawn as follows:

1. The microseismic monitoring carried out in the left bank slope of Jinping I hydropower station highlighted stability analysis of the slope, especially the deformation of deep rock mass. The monitoring results provide invaluable information about the tempo-spatial distribution and characteristics of excavation/grouting-induced microseismicity. The regions characterized by seismic clusters show strong correlation with pre-existing geological structures, especially faults or fractures inside the rock slope. The current microseismicity occurred mainly along the slope of dam abutment where excavation was nonproductive. One proper explanation for this phenomenon is that microseismicity is caused by excavation at the dam foundation and grouting inside the slope. Thus, microseismic events could reveal the processes of initiation, development and expansion of micro-fractures inside rock slope, which could delineate the regions of potential instability. Consequently, support measures for the slope could be proposed.
2. The study of microseismic monitoring on Dagangshan project focuses on precisely determining the volume of influence at the right bank slope. The results show that microseismic monitoring can not only provide invaluable information on the tempo-spatial distribution and characteristics of excavation-induced microseismicity, but also give an indication whether a particular known geological structures is seismically active or not. Planes of weakness defined by microseismic events may indicate previously unknown geological structures. Furthermore, the current microseismicity mainly occurred around the elevation 1180 m of the upstream slope, especially concentrating on the hanging wall of the fault XL316-1. This is predominantly attributed to continuous excavation of the shearing-resistance tunnels at 1120 m and 1150 m elevation. Seismic source locations thus show a strong correlation with structure elements on-site.
3. It can be concluded that the usefulness of microseismic monitoring stems from the fact that microcrackings are located by the seismic monitoring system wherever they occur and a 3-D picture of cracks can be obtained, unlike the 1-D or 2-D data obtained from conventional monitoring. It is not so much a short-term slope failure warning

technique, but rather a system for longer-term understanding of where and when rock failures are occurring in deep rock mass of rock slopes. Therefore, microseismic activity can be regarded as the precursor of surface movement and instability failure of the rock slope.

4. The microseismicity formation recorded in Jinping II project indicates that precursory microcracking exists in prior to most rockbursts, which can be captured by the microseismic monitoring system. Rock mass failure precursors can be detected by the microseismic monitoring system for rockburst prediction tens of or more than 100 meters away. The approximate range of rockbursts can be identified and delineated by clustering of seismic source locations. Precursors usually appeared a few days before the rockburst event in terms of time. Due to the occurrence of rockburst is related to excavation progress, the exact time of rockburst can hardly be predicted although the location of rockburst may be determined in advance.

The rock mechanics and rock engineering problems are increasingly complex as the engineering scale of rock excavation at large-scale hydropower projects becomes larger and larger in China. Consequently, as a supplement and extension of traditional rock monitoring technique, high-precision microseismic monitoring technology can be regarded as an effective tool to understand rock mass deformation in complex stress conditions and the corresponding possible hazard evolution mechanism.

5. References

Abdul-Wahed, M. K., Al Heib, M.,Senfaute, G., 2006. Mining-induced seismicity: Seismic measurement using multiplet approach and numerical modeling. International Journal of Coal Geology, 66: 137-147.

Cai, M.,Kaiser, PK., 2005. Assessment of excavation damaged zone using a micromechanics model. Tunnelling and Underground Space Technology, 20: 10.

Cook, N G W, 1964. The application of seismic techniques to problems in rock mechanics. International Journal of Rock Mechanics and Mining Science and Geomechanics Abstracts, 1: 169-179.

Ge, Maochen, 2005. Efficient mine microseismic monitoring. International Journal of Coal Geology, 64: 44-56.

Hirata, A., Kameoka, Y.,Hirano, T., 2007. Safety management based on detection of possible rock bursts by AE monitoring during tunnel excavation. Rock Mechanics And Rock Engineering, 40: 563-576.

Hudyma, M R. 2008. Analysis and interpretation of clusters of seismic events in mines. Department of civil and resource engineering, University of Western Australia.

Jiang, F.X. , Yang, S.H., Cheng, Y.H., Zhang, X.M., Mao, Z.Y,Xu, F.J, 2006. A study on microseismic monitoring of rock burst in coal mine. Chinese Journal of Geophysics, 49(5): 1511-1516.

Kaiser, P.K, Vasak,P, Suorineni,F T, 2005. New dimensionals in seismic data interpretation with 3-D virtual reality visualtion for burst-prone mines. In New dimensionals in seismic data interpretation with 3-D virtual reality visualtion for burst-prone mines, eds. Y Potvin and M Hudyma, Controlling seismic risk- Proceedings of sixth international symposium on rockburst and seismicity in mines, 33-45. Nedlands: Australian Center for Geomechanics.

Lynch, R A,Mendecki, A J. 2001. High-resolution seismic monitoring in mines. In High-resolution seismic monitoring in mines, eds. G Van Aswegen, R J Durrheim and W D Ortleep, Proceedings of fifth international symposium on rockburst and seismicity in mines, 19-24. Johannesburg: The South African Institute of Mining and Metallurgy.

Lynch, R.A., Wuite, R., Smith, B.S.,Cichowicz, A. 2005. Micro-seismic monitoring of open pit slopes. In Micro-seismic monitoring of open pit slopes, eds. Potvin.Y and Hudyma.M, Proceeding of the 6th Symposium on Rockbursts and Seismicity in Mines, 581-592. Perth, Australia: ACG.

Mendecki, A J. 1997. Keynote leeture: Principle of monitoring seismic rockmass response to mining. In Keynote leeture: Principle of monitoring seismic rockmass response to mining, ed. S J Gibowiez, Proceedings of the fourth international symposium on rockbursts and seismieity in mines, 69-80. Rotterdam:A.A.Balkema.

Mendecki, A J. 2000. Data-driven understanding of seismic rockmass response to mining. In Data-driven understanding of seismic rockmass response to mining, eds. G Van Aswegen, R J， Durrheim and W D Ortleep, Proceedings of fifth international symposium on rockburst and seismieity in mines l-9. Johannesburg: The South African Institute of Mining and Metallurgy.

Milev, A M, Spottiswoode, S M,Rorke, A J, 2001. Seismic monitoring of a simulated rock burst on a wall of an underground tunnel. Journal Of The South African Institute Of Mining And Metallurgy, 101: 8.

Potvin, Y,Hudyma, M R. 2001. Keynote address: Seismic monitoring in highly mechanized hardrock mines in Canada and Australia. In Keynote address: Seismic monitoring in highly mechanized hardrock mines in Canada and Australia, eds. G Van Aswegen, R J Durrheim and W D Ortleep, Proceedings of fifth international symposium on rockburst and seismicity in mines, 267-280. Johannesburg: The South African Institute of Mining and Metallurgy.

Shumila, V,Trifu, CI. 2009. Event mechanism analysis for seismicity induced by a controlled collapse in field II at Ocnele Mari, Romania. In Event mechanism analysis for seismicity induced by a controlled collapse in field II at Ocnele Mari, Romania., ed. CA Tang, Proceedings of the 7th international symposium on rockburst and seismicity in mines, Controlling seismic hazard and sustainable development of deep mines (RaSiM7), p.1091–1104. Dalian, China: New York: Rinton Press.

Tang, C.A., Wang, J.M.,Zhang, J.J., 2011. Preliminary engineering appliction of microseismic monitoring technique to rockburst prediction in tunneling of Jinping II project. Journal of Rock Mechanics and Geotechnical Engineering, 2: 16.

Tezuka, K.,Niitsuma, H., 2000. Stress estimated using microseismic clusters and its relationship to the fracture system of the Hijiori hot dry rock reservoir. Engineering Geology, 56: 47-62.

Trifu, CI，,Shumila, V. , 2010. Microseismic monitoring of a controlled collapse in Field II at Ocnele Mari，Romania. Pure And Applied Geophysics, 16: 15.

Urbancic, T.I.,Trifu, C.I., 2000. Recent advances in seismic monitoring technology at Canadian mines. Journal Of Applied Geophysics, 45: 225-237.

Xu, N W, Tang, C A, Li, H,Liang, Z Z, 2011a. Excavation-induced microseismicity: microseismic monitoring and numerical simulation. Journal of Zhejiang University-Science A, In press.

Xu, N W, Tang, C A, Li, H,Wu, S H, 2011b. Optimal design of microseismic monitoring networking and error analysis of seismic source location for rock slope. Open Civil Engineering Journal, 5.

Xu, N. W., Tang, C. A., Li, L. C., Zhou, Z., Sha, C., Liang, Z. Z.,Yang, J. Y., 2011c. Microseismic monitoring and stability analysis of the left bank slope in Jinping first stage hydropower station in southwestern China. International Journal Of Rock Mechanics And Mining Sciences, 48: 950-963.

Xu, N.W., Tang, C. A., Sha, C., Liang, Z. Z., Yang, J.Y,Zou, Y.Y, 2010. Microseismic monitoring system establishment and its engineering applications to left bank slope of Jinping I Hydropower Station. Chinese Journal of Rock Mechanics and Engineering, 29: 915-925.

Zhong, DH, Li, MC, Song, LG,Wang, G. , 2006. Enhanced NURRS modeling and visualization for large 3D geoengineering applications: An example from the Jinping first–level hydropower engineering project, China. Computers & Geosciences, 32: 13.

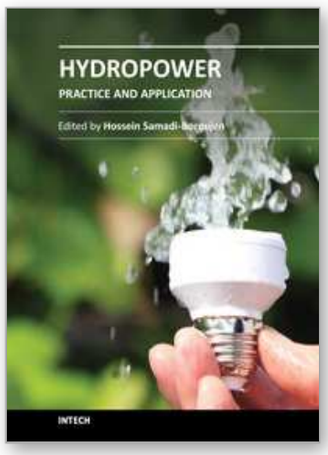

Hydropower - Practice and Application
Edited by Dr. Hossein Samadi-Boroujeni

ISBN 978-953-51-0164-2
Hard cover, 320 pages
Publisher InTech
Published online 09, March, 2012
Published in print edition March, 2012

Hydroelectric energy is the most widely used form of renewable energy, accounting for 16 percent of global electricity consumption. This book is primarily based on theoretical and applied results obtained by the authors during a long time of practice devoted to problems in the design and operation of a significant number of hydroelectric power plants in different countries. It was preferred to edit this book with the intention that it may partly serve as a supplementary textbook for students on hydropower plants. The subjects being mentioned comprise all the main components of a hydro power plant, from the upstream end, with the basin for water intake, to the downstream end of the water flow outlet.

INTECH
open science | open minds

InTech Europe
University Campus STeP Ri
Slavka Krautzeka 83/A
51000 Rijeka, Croatia
Phone: +385 (51) 770 447
Fax: +385 (51) 686 166
www.intechopen.com

InTech China
Unit 405, Office Block, Hotel Equatorial Shanghai
No.65, Yan An Road (West), Shanghai, 200040, China
中国上海市延安西路65号上海国际贵都大饭店办公楼405单元
Phone: +86-21-62489820
Fax: +86-21-62489821

IntechOpen